Published in final edited form as:
J Neurosci Methods. 2009 November 15; 184(2): 199–205. doi:10.1016/j.jneumeth.2009.08.002.

Insertion shuttle with carboxyl terminated self-assembled monolayer coatings for implanting flexible polymer neural probes in the brain

Takashi D. Yoshida Kozai[1] and **Daryl R. Kipke**[2,*]

[1]University of Michigan, 1101 Beal Avenue, 2110 Lurie Biomedical Engineering, Ann Arbor, MI 48109, USA. Tel.: +1 720 984 7016; fax: +1 734 647 4834.

[2]University of Michigan, 1101 Beal Avenue, 2212 Lurie Biomedical Engineering, Ann Arbor, MI 48109, USA.

Abstract

Penetrating microscale microelectrodes made from flexible polymers tend to bend or deflect and may fail to reach their target location. The development of flexible neural probes requires methods for reliable and controlled insertion into the brain. Previous approaches for implanting flexible probes into the cortex required modifications that negate the flexibility, limit the functionality, or restrict the design of the probe. This study investigated the use of an electronegative self-assembled monolayer (SAM) as a coating on a stiff insertion shuttle to carry a polymer probe into the cerebral cortex, and then the detachment of the shuttle from the probe by altering the shuttle's hydrophobicity.

Polydimethylsiloxane (PDMS) and polyimide probes were inserted into an agarose in vitro brain model using silicon insertion shuttles. The silicon shuttles were coated with a carboxyl terminal SAM. The precision of insertion using the shuttle was measured by the percentage displacement of the probe upon shuttle removal after the probe was fully inserted. The average relative displacement of polyimide probes inserted with SAM-coated shuttles was (1.0 ± 0.66)% of the total insertion depth compared to (26.5 ± 3.7)% for uncoated silicon shuttles. The average relative displacement of PDMS probes was (2.1 ± 1.1)% of the insertion depth compared to 100% (complete removal) for uncoated silicon shuttles. SAM-coated shuttles were further validated through their use to reliably insert PDMS probes in the cerebral cortex of rodents. This study found that SAM-coated silicon shuttles are a viable method for accurately and precisely inserting flexible neural probes in the brain.

Keywords

Microelectrode; Surgical technique; Cortex; Implant

*Corresponding author. Tel.: +1 734 764 3716; fax: +1 734 647 4834. tkozai@umich.edu (T.D.Y. Kozai), dkipke@umich.edu (D.R. Kipke).

Conflict of interest

D. Kipke has a significant financial and leadership interest in NeuroNexus Technologies.

1. Introduction

There is an ongoing need for higher fidelity and longer lasting implantable microscale neural interfaces for recording and stimulation both in scientific and emerging clinical applications (Brown et al., 1998; Fetz and Finocchio, 1975; Gage et al., 2005; Georgopoulos et al., 1986; Kargo and Nitz, 2003; Kipke et al., 2008; Nicolelis et al., 2003; Schwartz and Moran, 2000; Taylor et al., 2002). Multiple groups have reported wire-, silicon-, and polymer-based implantable neural probe technologies at various stages of development that are advancing neural interface capabilities across many dimensions, including channel count, site and substrate materials, and ability to precisely target locations in neocortex, deep brain, and spinal cord (Bartels et al., 2008; Hetke and Anderson, 2002; McCreery et al., 2006; McNaughton et al., 1983; Motta and Judy, 2005; Musallam et al., 2007; Neves and Ruther, 2007; Nicolelis et al., 2003; Nordhausen et al., 1996; Rennaker et al., 2005; Schwartz, 2004; Wise et al., 2004). For chronically implanted probes, one challenge is to improve and/or control the degree to which the probe integrates with the surrounding tissue to meet particular performance requirements, such as high signal-to-noise ratio and long-term stability (Liu et al., 2006; Nicolelis et al., 2003; Polikov et al., 2005; Rousche and Normann, 1998; Schwartz et al., 2006; Williams et al., 1999). Computer models and experimental studies of the probe–tissue interface suggest that flexible and soft probes that approach the brain's bulk material characteristics may help to minimize micromotion between the probe and surrounding tissue (Biran et al., 2005; Cheung et al., 2007; Gilletti and Muthuswamy, 2006; Kim et al., 2004; LaPlaca et al., 2005; Lee et al., 2005; Neary et al., 2003; Subbaroyan et al., 2005). To this end, biocompatible polymers such as polyimide, Parylene-C, and PDMS have been employed for flexible probes, although they have not been extensively tested for long-term stability for neural recordings (Rousche et al., 2001; Weiland et al., 2005). Additionally, advanced types of probe architectures with sub-cellular sized features have been shown to elicit smaller reactive tissue responses (Metz et al., 2004; Rousche et al., 2001; Seymour and Kipke, 2007). Both mechanisms may facilitate improved long-term tissue integration, and thus long-term function of the device.

However, there is an interesting conflict between a probe's flexibility, softness, and feature size that are hypothesized to be important for long-term tissue integration and the largely opposite mechanical characteristics that are thought to be important for reliable and minimally damaging insertion in the brain. The viscoelastic and inhomogeneous properties of the brain make the mechanics of probe insertion a complex process involving device size, sharpness, stiffness, and the target area of the brain. There is not a consensus on optimal insertion techniques, although it is a function of many parameters. Empirical evidence suggests that stiff, sharp, and straight probes should be inserted relatively fast, but under control for a minimally damaging insertion (Bjornsson et al., 2006; Edell et al., 1992; Johnson et al., 2007).

In particular, thin-film, microscale polymer probes that have desirable flexibility for long-term implantation tend to buckle before penetrating the pia mater or deflect while being directed to the target area. Existing methods to suitably strengthen polymer probes for insertion restrict the design of the probe, limit its functionality, or negate its flexibility. One approach is to integrate a rigid insertion device during fabrication (O'Brien et al., 2001), however this technique restricts probe design and presents challenges in precise implantations. Another approach is to coat a flexible or small probe with stiff biodegradable polymers or crystals (Foley et al., 2006; Suzuki et al., 2003), but these present significant challenges to achieve the appropriate stiffness, reproducibility, and sharpness in a small conformal coating. An alternative approach is to create channels in the substrate which can be filled with stiff biodegradable polymers or crystals (Takeuchi et al., 2004). These electrode designs require a larger fluid channel to fill with biodegradable material to reach a

critical stiffness for insertion. This larger channel then results in a larger implanted footprint, potentially creating more damage. Other methods include a polymer substrate integrated with a stiff silicon backbone (Lee et al., 2004), but this negates the flexibility of the polymer substrate.

Our development strategy is to find ways to uncouple the requirements of a long-term implanted probe from the specifications needed for minimally damaging insertion. Our approach involves an assembly having a soft, flexible, small implantable probe and a separate thin stiff, sharp, straight insertion shuttle that carries the probe into the brain and is then removed. However, polymer probes stick to metallic and silicon surfaces through hydrophobic interactions, causing a polymer probe to be carried out of the brain when the insertion shuttle is removed. Our innovative approach is to use a highly hydrophilic, electronegative, self-assembled monolayer (SAM) coating on the shuttle. When the assembly is in the brain, the hydrophilic-coated shuttle attracts water molecules to the probe-shuttle surface causing the polymer probe to separate from the shuttle. A study that shows that 'stab wounds' from silicon microelectrodes do not cause noticeable neuronal loss (Biran et al., 2005), suggests that the incremental damage associated with the shuttle would be expected to have negligible negative effects to the tissue. This two-component approach decouples the biocompatibility, flexibility, and neural integration requirements of probes from the contradictory mechanical and handling requirements for reliably inserting the probe into the brain.

In this study, we developed a novel carboxylic acid terminal SAM coating for the insertion shuttle and then validated the insertion shuttle polymer probe system through *in vitro* and *in vivo* testing. 11-Mercaptoundecanoic acid has been used for various SAM applications for *in vitro* cell cultures and *in vivo* and has indications of good biocompatibility (Huang et al., 2008; Lan et al., 2005; Romanova et al., 2006; Tidwell et al., 1997; Xiao et al., 2007), particularly for short term applications. We quantified the accuracy and precision of insertion of polymer probes using SAM-coated shuttles into a gel model of the brain and also into rat cortex. We found the SAM-coated shuttle to be an effective and reliable insertion tool for polymer probes that is validated for further development.

2. Methods

2.1. Probe insertion shuttles

The probe insertion shuttles were conventional, "Michigan"-style thin-film silicon-substrate neural probes (Drake et al., 1988; Hetke and Anderson, 2002) modified to have a SAM surface to enable release of polymer probes. These shuttles had one penetrating shank 15 μm thick, 1 cm long, and 400 μm wide gradually tapering to the tip. Each shuttle was mounted onto a blank printed circuit board (PCB) and attached to a bare silicon wafer using Kapton tape. The flat surface of the silicon shuttles and wafer were then coated together with 100 Å titanium, followed by 1000 Å gold via resistive evaporation. The Kapton tape was removed, and then the gold-coated shuttles and wafer were immersed together in 1 mM ethanolic solution of 11-mercaptoundecanoic acid for 48 h. They were then rinsed twice in ethanol for 5 min, followed by a 0.1-M HCl rinse, and then a de-ionized (DI) water rinse. The SAM-coated shuttles and wafer were then stored in ethanol for up to 1 week before use. A 1 cm × 1 cm SAM-coated wafer fragment was inspected and compared to a 1 cm × 1 cm gold-coated wafer using infrared spectroscopy on a Magna 550 spectrometer (Nicolete) to confirm that the SAM was present on the gold surface. Fig. 1 shows two representative IR spectra of the uncoated and SAM-coated silicon fragments. The spectrum of the SAM-coated shuttle has three peaks characteristic of the SAM: two peaks at wavenumbers 2919 cm^{-1} and 2851 cm^{-1} related to the hydrocarbon backbone of 11-mercaptoundecanoic acid and a peak at 1714 cm^{-1} indicating the carboxyl group.

2.2. Flexible neural probes

Two types of flexible polymer probes were used. The first type was a thin-film polyimide-substrate probe obtained from NeuroNexus Technologies, Inc. (Ann Arbor, MI, USA). These probes had a single penetrating shank 12.5 μm thick, 196 μm wide and 1.2 cm long with a pointed tip. The probes also had 12 exposed metal electrode sites and buried thin-film metal traces that were not used in this study.

The second type was a PDMS-substrate probe made in our laboratory. The fabrication process started with deposition of a 1-μm thick sacrificial aluminum layer through e-beam evaporation (Denton Vacuum) onto a silicon wafer. This was followed by spin coating of an epoxy based, negative photoresist SU-8 2075 to a thickness of 100 μm. The photoresist layer was patterned in UV light. These probes were patterned to be 200 μm wide and 1.5 cm long with a pointed tip. The patterned SU-8 layer served as a mold for the PDMS.

PDMS (Sylgard 184, Dow Corning) was prepared by mixing pre-polymer and curing agent in a 10:1 ratio. The mixture was degassed in a vacuum chamber to remove bubbles and spun coated onto the silicon wafer. Excess PDMS was removed using a clean blade. The PDMS was cured at 150 °C for 12 h, followed by residual PDMS removal through etching with CF_4:O_2 (3:1) plasma for 3–5 min. The sacrificial aluminum layer was removed through etching with potassium hydroxide (KOH) solution. The individual PDMS probes were then manually removed from the wafer using microforceps. The released probes were rinsed in ethanol, DI water, and dried in air.

2.3. Insertion technique and quantification

Individual polymer probes of either type were placed by hand onto the SAM-coated surface of the insertion shuttle using microforceps 2–5 min prior to insertion. The probe was placed such that it did not extend past the tip of the insertion shuttle and its edges rested within the edges of the shuttle (Figs. 2A and 3). When necessary, a droplet of 70% ethanol was temporarily placed onto the SAM-coated surface of the shuttle to help positioning of the polymer probe onto the shuttle, and then the shuttle assembly was dried in air. This assembly was then manually positioned and inserted using microforceps into either a gel model of the brain or *in vivo* rat brain. After the assembly was inserted, the polymer probe was peeled from the insertion shuttle to the surface of the gel or brain as shown in Fig. 2B. A drop of artificial cerebrospinal fluid (ACSF) (Harvard Apparatus) was used to help detach the polymer probe from the insertion shuttle as illustrated in Fig. 2C. To ensure that the probe and shuttle are detached, additional droplets of ACSF may be applied until a meniscus can be observed between the probe and the shuttle or until the craniotomy is filled. After the polymer probe detached from the shuttle, the shuttle was manually grasped using microforceps and slowly removed from the gel or brain.

Probe insertions using both types of polymer probes were quantified using a gel model of the bulk mechanical characteristics of the cortex under controlled conditions. The transparent gel model consisted of 250 ml 0.5% agarose in phosphate buffered saline (PBS) with a thin layer of PBS on the surface of the agarose (Chen et al., 2002, 2004; Theer et al., 2003). Agarose of this concentration has similar elastic and shear moduli as brain tissue (Barrangou et al., 2006; Gefen et al., 2003; Hamhaber et al., 2003; Normand et al., 2000; Prange and Margulies, 2002; Thibault and Margulies, 1998) while allowing visualization of probes within the gel. Blue dye or red dye was used to contrast the clear PDMS probes from the gel for imaging purposes. Each shuttle-probe assembly was inserted into the agarose using the previously described technique. High-resolution digital images were then obtained of the assembly and/or the released probe in the gel model using a fixed-position camera (Fujifilm FinePix S2 Pro with a Sigma Ex 105 mm 1:2.8 D Macro Lens at full zoom) a

known distance from the model. The resolution of each image was calculated by dividing the known width of the probe in microns by the measured width of the probe from the images in pixels. The average resolution of each image was 5.3 μm/pixel. Probe penetration distance was measured immediately after insertion with the shuttle in place and again following the removal of the shuttle. The accuracy of implantation was evaluated by calculating the absolute displacement magnitude of the probe tip from probe insertion to shuttle removal. Precision was measured from the standard error. Statistical significance was calculated using a *T*-test.

Additionally, PDMS probes were manually inserted into rat cerebral cortex to validate the insertion technique in a typical experimental preparation. Adult male Sprague–Dawley rats (Charles River Laboratories) weighing 300–350 g were prepared for cortical implants using previously established methods (Ludwig et al., 2006; Vetter et al., 2004). The animal was anesthetized with a mixture of 50 mg/mL ketamine, 5 mg/mL xylazine, and 1 mg/mL of acepromazine administered intraperitoneally with an initial dosage of 0.125 mL/100 g of body weight and regular updates of ketamine. The depth of anesthesia was regulated by monitoring heart rate and blood oxygen saturation. The animal was placed into a stereotaxic frame and a 3 mm by 3 mm craniotomy was made over the primary motor cortex in each hemisphere. The dura was incised and resected. Sterile saline was used to keep the brain surface moist throughout the procedure.

Controlled probe implantations involved lowering a polymer probe inserted shuttle through the craniotomy and into brain tissue. The shuttle and polymer probe were held across the PCB with a micro-alligator clip (BU-34C, Mueller Electric Company, Cleveland, OH). A piezoelectric actuator (M-230.25, Physik Instrumente, Karlsruhe, Germany) mounted to the stereotaxic frame guided insertions by means of a dc-motor controller (C-890.PS, Physik Instrumente). The insertion tool system had a maximum velocity of 1.2 mm/s with a spatial range of 25 mm with a resolution of 4.6 nm monitored by Hall effect transducers. During the first insertion trial, the shuttle was positioned until the tip of the shuttle touched the surface of the brain and then advanced at various speeds of 1 mm/s, 50 μm/s, 5 μm/s, and 1 μm/s for 5 mm such that the polymer probe penetrated the tissue 2–3 mm. Subsequently, arrays were inserted into brain tissue 5 times at each speed with horizontal separations of at least 400–500 μm. All procedures complied with the United States Department of Agriculture guidelines for the care and use of laboratory animals and were approved by the University of Michigan Committee on Use and Care of Animals.

3. Results

3.1. Characterization of insertion shuttle using gel models

Polymer probes were placed onto the insertion shuttle (Fig. 3) and inserted into separate gel tissue phantoms. Immediately after insertion with the shuttle still in place, the polymer probe penetration distance was measured. A second measurement was taken following the removal of the shuttle. Displacement of ten polyimide probes using ten SAM-coated insertion shuttles was significantly less than that of non-SAM-coated shuttles ($p < 0.0001$) (Fig. 4A and B, Table 1). The average relative probe displacement was (1.0 ± 0.66)% (mean ± standard error) of the insertion distance or 85 ± 55 μm displacement for an average target depth of t_{target} = 8830 μm insertion. On average the net final position of the polymer probes after the shuttle removal was t_{target} + 23 μm. For ten polyimide probes inserted into separate gel models using ten insertion shuttles without SAM coating (Fig. 4A and B, Table 1), the average relative displacement was (26.5 ± 3.7)% of the insertion distance or 2365 ± 334 μm displacement for an average t_{target} = 8830 μm insertion. On average the net final position was t_{target} + 2365 μm.

Additionally, when reusing a single SAM-coated shuttle, displacement of ten polyimide probes was significantly less than that of non-SAM-coated shuttles ($p < 0.0001$) (Table 1). The average relative probe displacement was (3.3 ± 1.5)% of the implantation distance or 299 ± 135 μm displacement for an average t_{target} = 8270 μm insertion. On average the final position was t_{target} + 57 μm. After the first insertion, there was an increase in displacement. However, displacement remained steady for the remaining nine insertions. While it is possible to reuse a SAM-coated shuttle, a freshly coated shuttle evokes less than one-half the displacement of a used shuttle.

Displacement of ten PDMS probes using ten SAM-coated insertion shuttles was significantly less than that of non-SAM-coated shuttles ($p < 0.0001$) (Fig. 4D and E, Table 1). The average relative probe displacement was (2.1 ± 1.1)% of the implantation distance or 167 ± 79 μm displacement for an average t_{target} = 8280 μm insertion. On average, the net final position was t_{target} + 71 μm. For ten PDMS probes inserted using ten insertion shuttles without SAM coating, all ten probes were completely explanted for an average t_{target} = 8130 μm implantation.

3.2. In vivo validation of insertion shuttle

SAM-coated insertion shuttles were validated for inserting flexible polymer probes into the brain. Six PDMS probes were successfully implanted into the motor cortex of three male, adult rats using SAM-coated insertion shuttles (Fig. 5). Removal of the SAM-coated insertion shuttle did not cause visible displacement of the PDMS probes, while removal of the non-coated insertion shuttle caused complete removal of the PDMS probes (see Supplementary Video). PDMS probes could not be inserted into cortex without the insertion shuttle because of their flexibility. When using a controlled insertion technique with a stereotaxic frame guided piezoelectric actuator, polymer probes were successfully inserted each trial at 1 mm/s, 50 μm/s, 5 μm/s, and 1 μm/s.

4. Discussion

4.1. Probe insertion and displacement

This is the first time SAM modification of a silicon insertion shuttle has been demonstrated to enable flexible polymer devices to enter soft tissue with subsequent removal of the shuttle resulting in negligible displacement of the polymer device. We hypothesize that the polymer probe is held to the surface of the insertion shuttle through electrostatic interactions, therefore it is important that the probe lies flat on the shuttle. Polyimide probes showed improved reliability and controllability of insertion when coupled with the SAM modified shuttle. The PDMS probes were too flexible to enter the cerebral cortex alone. The SAM modified shuttle enabled implantation of PDMS probes and subsequent removal of the shuttle.

Occasionally the PDMS probe would slide along the insertion shuttle during insertion into agarose. Ensuring the PDMS probe and shuttle were dry, gripping closer to the bottom of the PCB with forceps, and inserting in a straight controlled fashion ensured successful implantation of the PDMS probe. Mounting a shorter silicon shuttle substrate onto the PCB or mounting the polymer probe tip closer to the base of the shuttle can achieve similar results without directly gripping the silicon substrate with forceps. Once the tip of the polymer probe was inserted into the tissue or tissue phantom, the probe would not separate until it was released with a drop of saline, even with manual insertions (~1 mm/s). A controlled insertion technique can enable slower insertions. Additionally, a precise parallel alignment of the probe was not necessary along the axis of the shuttle so long as the polymer probe lay within the edges of the shuttle. If the probe laid outside of the edges of the shuttle,

particularly near the tip, there is a chance that the polymer probe can get caught on the tissue during insertion, particularly for PDMS probes. Therefore, the shuttle should be at least as wide as the polymer probe. While a shuttle with the same size as a flexible probe will reduce the initial insertion footprint, it may increase difficulty in probe alignment.

4.2. Release mechanism model

Solid materials such as polymers and silicon adhere to each other in an aqueous environment due to surface energies (Johnson et al., 1971). In the presence of a thin aqueous meniscus, two hydrophobic substrates in contact, such as glass and metal, demonstrate strong adhesive forces (Mcfarlane and Tabor, 1950). It is further understood that this adhesive force is formed by a convex-shaped menisci which creates a lower pressure inside the meniscus resulting in an intrinsic attractive force, and during separation the viscosity of the liquid causes an additional attractive force (Cai and Bhushan, 2008a,b). In the case of a polymer probe and silicon shuttle in the brain, this thin aqueous meniscus is formed at the triple junction between polymer, silicon, and extracellular fluid.

For hydrophilic surfaces, meniscus forces have been well characterized (Cai and Bhushan, 2008a). A concave-shaped meniscus is formed driving the liquid between the two surfaces in a phenomena described as capillary action, which leads to a separation of the two surfaces in an aqueous solution. Therefore, separation can be achieved by converting one of the hydrophobic surfaces (the shuttle) to a highly hydrophilic surface with a coating such that the meniscus force along the new hydrophilic surface overcomes the meniscus force along the hydrophobic probe surface. 11-Mercaptoundecanoic acid coated surfaces become highly electronegative and hydrophilic (Yan et al., 1997), and can be used to coat the shuttle for this purpose.

Finally, the polymer probe seems to rarely separate during insertion into hydrated tissue. The surface tension and atomic level roughness on the surface of the polymer probe and shuttle junction may prevent fluid in the tissue from separating the bundle during implantation (Denkov et al., 1999; Grassi et al., 2006). This may be why it is necessary to peel the polymer probe from the SAM-coated shuttle at the back end and then add a droplet of ACSF to separate the shuttle from the probe after implantation.

4.3. Future directions

The insertion shuttle could be modified to be narrower and thicker to improve handling and decrease the chance of fracture within the tissue. 15 μm thick shuttles are unable to penetrate the dura, however, 50 μm thick silicon shuttles or 40 μm thick C1095 spring steel shuttles can penetrate the dura, and may enable flexible polymer probe insertions through the dura as well as improve ease of use. Insertion shuttles also could be made from stiffer materials such as titanium or tungsten for insertion of probes into sub-cortical structures. However, a larger shuttle would evoke greater tissue damage during insertion. This damage may be minimal in chronic implantations since the shuttle is immediately removed similar to a stab wound (Biran et al., 2005). Additionally, sustained tissue responses have been shown to be similar for two different style probes with an order of magnitude different cross-sectional area (Szarowski et al., 2003), which suggests that a slightly larger shuttle may not create a noticeable difference in tissue response. However, the specific relationship between shuttle size and stab wound on chronic tissue response has not been determined. Channels or grooves on the surface of the insertion shuttle could improve separation of the PDMS probe from the insertion shuttle. Additionally, the shape of the shuttle tip could be optimized to reduce mechanical trauma to the tissue during insertion. Incorporating this shuttle approach for controlled insertion techniques with motorized insertions may lead to minimally damaging insertions (Bjornsson et al., 2006; Johnson et al., 2007). Future investigations also

include examining adhesion forces between the polymer probe and shuttle before and after release.

Many polymers are currently available for the fabrication of microelectrodes. These polymers have unique characteristics such as flexibility, structural stability, electrical properties, surface chemistry, and biocompatibility. Flexible microelectrode technologies have been underdeveloped in part because investigators lack a precise and efficient method to implant and validate these flexible microelectrodes *in vivo*. The ability to quickly and precisely implant polymer probes into the cortex will promote future polymer microelectrode development. Furthermore, microelectrode geometries (Szarowski et al., 2003), tip shapes, and insertion speeds influence mechanical and chemical strain on the tissue (Bjornsson et al., 2006; Johnson et al., 2007). Uncoupling the biocompatibility and neural integration requirements of probes from the mechanical and handling requirements for reliably inserting the probe into the brain can allow a new degree of freedom to explore flexible microelectrode designs. Microelectrode tip shape, anchor, stiffness, size, and surface chemistry can be designed for biocompatibility independent of the requirements to minimize insertion trauma. This can in turn open opportunities for innovative microelectrode designs that focus solely on improving the chronic device–tissue interface.

Supplementary Material

Refer to Web version on PubMed Central for supplementary material.

Acknowledgments

The author thanks Jeyakumar Subbaroyan for his help in the clean room and for performing the surgeries. This research is supported by Center for Neural Communication Technology, a P41 Resource Center funded by the National Institute of Biomedical Imaging and Bioengineering (NIBIB, P41 EB002030) and supported by the National Institutes of Health (NIH).

Appendix A. Supplementary data

Supplementary data associated with this article can be found, in the online version, at doi:10.1016/j.jneumeth.2009.08.002.

References

Barrangou LM, Drake M, Daubert CR, Foegeding EA. Textural properties of agarose gels. II. Relationships between rheological properties and sensory texture. Food Hydrocolloids. 2006; 20:196–203.

Bartels J, Andreasen D, Ehirim P, Mao H, Seibert S, Wright EJ, et al. Neurotrophic electrode: method of assembly and implantation into human motor speech cortex. J Neurosci Methods. 2008; 174:168–176. [PubMed: 18672003]

Biran R, Martin DC, Tresco PA. Neuronal cell loss accompanies the brain tissue response to chronically implanted silicon microelectrode arrays. Exp Neurol. 2005; 195:115–126. [PubMed: 16045910]

Bjornsson CS, Oh SJ, Al-Kofahi YA, Lim YJ, Smith KL, Turner JN, et al. Effects of insertion conditions on tissue strain and vascular damage during neuroprosthetic device insertion. J Neural Eng. 2006; 3:196–207. [PubMed: 16921203]

Brown EN, Frank LM, Tang D, Quirk MC, Wilson MA. A statistical paradigm for neural spike train decoding applied to position prediction from ensemble firing patterns of rat hippocampal place cells. J Neurosci. 1998; 18:7411–7425. [PubMed: 9736661]

Cai S, Bhushan B. Meniscus and viscous forces during separation of hydrophilic and hydrophobic surfaces with liquid-mediated contacts. Mater Sci Eng R-Rep. 2008a; 61:78–106.

Cai S, Bhushan B. Viscous force during tangential separation of meniscus bridges. Philos Mag. 2008b; 88:449–461.

Chen ZJ, Broaddus WC, Viswanathan RR, Raghavan R, Gillies GT. Intraparenchymal drug delivery via positive-pressure infusion: experimental and modeling studies of poroelasticity in brain phantom gels. IEEE Trans Biomed Eng. 2002; 49:85–96. [PubMed: 12066887]

Chen ZJ, Gillies GT, Broaddus WC, Prabhu SS, Fillmore H, Mitchell RM, et al. A realistic brain tissue phantom for intraparenchymal infusion studies. J Neurosurg. 2004; 101:314–322. [PubMed: 15309925]

Cheung KC, Renaud P, Tanila H, Djupsund K. Flexible polyimide microelectrode array for in vivo recordings and current source density analysis. Biosens Bioelectron. 2007; 22:1783–1790. [PubMed: 17027251]

Denkov ND, Cooper P, Martin JY. Mechanisms of action of mixed solid-liquid antifoams. 1. Dynamics of foam film rupture. Langmuir. 1999; 15:8514–8529.

Drake KL, Wise KD, Farraye J, Anderson DJ, BeMent SL. Performance of planar multisite microprobes in recording extracellular single-unit intracortical activity. IEEE Trans Biomed Eng. 1988; 35:719–732. [PubMed: 3169824]

Edell DJ, Toi VV, McNeil VM, Clark LD. Factors influencing the biocompatibility of insertable silicon microshafts in cerebral cortex. IEEE Trans Biomed Eng. 1992; 39:635–643. [PubMed: 1601445]

Fetz EE, Finocchio DV. Correlations between activity of motor cortex cells and arm muscles during operantly conditioned response patterns. Exp Brain Res. 1975; 23:217–240. [PubMed: 810359]

Foley, CP.; Neeves, KB.; Saltzman, WM.; Olbricht, WL. Bioerodible scaffolds for implantable microfluidic probes in convection enhanced neural drug delivery; AIChE Annual Meeting; 2006.

Gage GJ, Ludwig KA, Otto KJ, Ionides EL, Kipke DR. Naive coadaptive cortical control. J Neural Eng. 2005; 2:52–63. [PubMed: 15928412]

Gefen A, Gefen N, Zhu Q, Raghupathi R, Margulies SS. Age-dependent changes in material properties of the brain and braincase of the rat. J Neurotrauma. 2003; 20:1163–1177. [PubMed: 14651804]

Georgopoulos AP, Schwartz AB, Kettner RE. Neuronal population coding of movement direction. Science. 1986; 233:1416–1419. [PubMed: 3749885]

Gilletti A, Muthuswamy J. Brain micromotion around implants in the rodent somatosensory cortex. J Neural Eng. 2006; 3:189–195. [PubMed: 16921202]

Grassi M, Cox B, Zhang X. Simulation of pin-reinforced single-lap composite joints. Compos Sci Technol. 2006; 66:1623–1638.

Hamhaber U, Grieshaber FA, Nagel JH, Klose U. Comparison of quantitative shear wave MR-elastography with mechanical compression tests. Magn Reson Med. 2003; 49:71–77. [PubMed: 12509821]

Hetke, JF.; Anderson, DJ. Silicon microelectrodes for extracellular recording. In: Finn, WE.; LoPresti, PG., editors. Handbook of neuroprosthetic methods. Boca Raton, FL: CRC; 2002.

Huang XL, Zhang B, Ren L, Ye SF, Sun LP, Zhang QQ, et al. In vivo toxic studies and biodistribution of near infrared sensitive Au-Au(2)S nanoparticles as potential drug delivery carriers. J Mater Sci Mater Med. 2008; 19:2581–2588. [PubMed: 17665103]

Johnson KL, Kendall K, Roberts AD. Surface energy and contact of elastic solids. Proc R Soc Lond Ser A: Math Phys Sci. 1971; 324:301–307.

Johnson MD, Kao OE, Kipke DR. Spatiotemporal pH dynamics following insertion of neural microelectrode arrays. J Neurosci Methods. 2007; 160:276–287. [PubMed: 17084461]

Kargo WJ, Nitz DA. Early skill learning is expressed through selection and tuning of cortically represented muscle synergies. J Neurosci. 2003; 23:11255–11269. [PubMed: 14657185]

Kim YT, Hitchcock RW, Bridge MJ, Tresco PA. Chronic response of adult rat brain tissue to implants anchored to the skull. Biomaterials. 2004; 25:2229–2237. [PubMed: 14741588]

Kipke DR, Shain W, Buzsaki G, Fetz E, Henderson JM, Hetke JF, et al. Advanced neurotechnologies for chronic neural interfaces: new horizons and clinical opportunities. J Neurosci. 2008; 28:11830–11838. [PubMed: 19005048]

Lan S, Veiseh M, Zhang M. Surface modification of silicon and gold-patterned silicon surfaces for improved biocompatibility and cell patterning selectivity. Biosens Bioelectron. 2005; 20:1697–1708. [PubMed: 15681184]

LaPlaca MC, Cullen DK, McLoughlin JJ, Cargill RS 2nd. High rate shear strain of three-dimensional neural cell cultures: a new in vitro traumatic brain injury model. J Biomech. 2005; 38:1093–1105. [PubMed: 15797591]

Lee H, Bellamkonda RV, Sun W, Levenston ME. Biomechanical analysis of silicon microelectrode-induced strain in the brain. J Neural Eng. 2005; 2:81–89. [PubMed: 16317231]

Lee KK, He JP, Singh A, Massia S, Ehteshami G, Kim B, et al. Polyimide-based intracortical neural implant with improved structural stiffness. J Micromech Microeng. 2004; 14:32–37.

Liu X, McCreery DB, Bullara LA, Agnew WF. Evaluation of the stability of intracortical microelectrode arrays. IEEE Trans Neural Syst Rehabil Eng. 2006; 14:91–100. [PubMed: 16562636]

Ludwig KA, Uram JD, Yang J, Martin DC, Kipke DR. Chronic neural recordings using silicon microelectrode arrays electrochemically deposited with a poly(3,4-ethylenedioxythiophene) (PEDOT) film. J Neural Eng. 2006; 3:59–70. [PubMed: 16510943]

McCreery D, Lossinsky A, Pikov V, Liu X. Microelectrode array for chronic deep-brain microstimulation and recording. IEEE Trans Biomed Eng. 2006; 53:726–737. [PubMed: 16602580]

Mcfarlane JS, Tabor D. Adhesion of solids and the effect of surface films. Proc R Soc Lond Ser A: Math Phys Sci. 1950; 202:224–243.

McNaughton BL, O'Keefe J, Barnes CA. The stereotrode: a new technique for simultaneous isolation of several single units in the central nervous system from multiple unit records. J Neurosci Methods. 1983; 8:391–397. [PubMed: 6621101]

Metz S, Bertsch A, Bertrand D, Renaud P. Flexible polyimide probes with microelectrodes and embedded microfluidic channels for simultaneous drug delivery and multi-channel monitoring of bioelectric activity. Biosens Bioelectron. 2004; 19:1309–1318. [PubMed: 15046764]

Motta PS, Judy JW. Multielectrode microprobes for deep-brain stimulation fabricated with a customizable 3-D electroplating process. IEEE Trans Biomed Eng. 2005; 52:923–933. [PubMed: 15887542]

Musallam S, Bak MJ, Troyk PR, Andersen RA. A floating metal microelectrode array for chronic implantation. J Neurosci Methods. 2007; 160:122–127. [PubMed: 17067683]

Neary JT, Kang Y, Willoughby KA, Ellis EF. Activation of extracellular signal-regulated kinase by stretch-induced injury in astrocytes involves extracellular ATP and P2 purinergic receptors. J Neurosci. 2003; 23:2348–2356. [PubMed: 12657694]

Neves, HP.; Ruther, P. The NeuroProbes project; 2007 annual international conference of the IEEE engineering in medicine and biology society; 2007. p. 6443-6445.

Nicolelis MA, Dimitrov D, Carmena JM, Crist R, Lehew G, Kralik JD, et al. Chronic, multisite, multielectrode recordings in macaque monkeys. Proc Natl Acad Sci U S A. 2003; 100:11041–11046. [PubMed: 12960378]

Nordhausen CT, Maynard EM, Normann RA. Single unit recording capabilities of a 100 microelectrode array. Brain Res. 1996; 726:129–140. [PubMed: 8836553]

Normand V, Lootens DL, Amici E, Plucknett KP, Aymard P. New insight into agarose gel mechanical properties. Biomacromolecules. 2000; 1:730–738. [PubMed: 11710204]

O'Brien, DP.; Nichols, TR.; Allen, MG. Flexible microelectrode arrays with integrated insertion devices. 14th IEEE international conference on micro electro mechanical systems. Technical Digest; 2001. p. 216-219.

Polikov VS, Tresco PA, Reichert WM. Response of brain tissue to chronically implanted neural electrodes. J Neurosci Methods. 2005; 148:1–18. [PubMed: 16198003]

Prange MT, Margulies SS. Regional, directional, and age-dependent properties of the brain undergoing large deformation. J Biomech Eng. 2002; 124:244–252. [PubMed: 12002135]

Rennaker RL, Ruyle AM, Street SE, Sloan AM. An economical multi-channel cortical electrode array for extended periods of recording during behavior. J Neurosci Methods. 2005; 142:97–105. [PubMed: 15652622]

Romanova EV, Oxley SP, Rubakhin SS, Bohn PW, Sweedler JV. Self-assembled monolayers of alkanethiols on gold modulate electrophysiological parameters and cellular morphology of cultured neurons. Biomaterials. 2006; 27:1665–1669. [PubMed: 16197993]

Rousche PJ, Normann RA. Chronic recording capability of the Utah Intracortical Electrode Array in cat sensory cortex. J Neurosci Methods. 1998; 82:1–15. [PubMed: 10223510]

Rousche PJ, Pellinen DS, Pivin DP, Williams JC, Vetter RJ, Kipke DR. Flexible polyimide-based intracortical electrode arrays with bioactive capability. IEEE Trans Biomed Eng. 2001; 48:361–371. [PubMed: 11327505]

Schwartz AB. Cortical neural prosthetics. Ann Rev Neurosci. 2004; 27:487–507. [PubMed: 15217341]

Schwartz AB, Cui XT, Weber DJ, Moran DW. Brain-controlled interfaces: movement restoration with neural prosthetics. Neuron. 2006; 52:205–220. [PubMed: 17015237]

Schwartz AB, Moran DW. Arm trajectory and representation of movement processing in motor cortical activity. Eur J Neurosci. 2000; 12:1851–1856. [PubMed: 10886326]

Seymour JP, Kipke DR. Neural probe design for reduced tissue encapsulation in CNS. Biomaterials. 2007; 28:3594–3607. [PubMed: 17517431]

Subbaroyan J, Martin DC, Kipke DR. A finite-element model of the mechanical effects of implantable microelectrodes in the cerebral cortex. J Neural Eng. 2005; 2:103–113. [PubMed: 16317234]

Suzuki, T.; Mabuchi, K.; Takeuchi, S. A 3D flexible parylene probe array for multichannel neural recording. Neural Engineering, Proceedings of the 1st international IEEE EMBS; 2003. p. 154-156.

Szarowski DH, Andersen MD, Retterer S, Spence AJ, Isaacson M, Craighead HG, et al. Brain responses to micro-machined silicon devices. Brain Res. 2003; 983:23–35. [PubMed: 12914963]

Takeuchi, S.; Yoshida, Y.; Ziegler, D.; Mabuchi, K.; Suzuki, T. Parylene flexible neural probe with micro fluidic channel. Mems 2004: 17th IEEE international conference on micro electro mechanical systems. Technical Digest; 2004. p. 208-211.

Taylor DM, Tillery SI, Schwartz AB. Direct cortical control of 3D neuroprosthetic devices. Science. 2002; 296:1829–1832. [PubMed: 12052948]

Theer P, Hasan MT, Denk W. Two-photon imaging to a depth of 1000 micron in living brains by use of a Ti:Al_2O_3 regenerative amplifier. Opt Lett. 2003; 28:1022–1024. [PubMed: 12836766]

Thibault KL, Margulies SS. Age-dependent material properties of the porcine cerebrum: effect on pediatric inertial head injury criteria. J Biomech. 1998; 31:1119–1126. [PubMed: 9882044]

Tidwell CD, Ertel SI, Ratner BD, Tarasevich BJ, Atre S, Allara DL. Endothelial cell growth and protein adsorption on terminally functionalized, self-assembled monolayers of alkanethiolates on gold. Langmuir. 1997; 13:3404–3413.

Vetter RJ, Williams JC, Hetke JF, Nunamaker EA, Kipke DR. Chronic neural recording using silicon-substrate microelectrode arrays implanted in cerebral cortex. IEEE Trans Biomed Eng. 2004; 51:896–904. [PubMed: 15188856]

Weiland JD, Liu W, Humayun MS. Retinal prosthesis. Annu Rev Biomed Eng. 2005; 7:361–401. [PubMed: 16004575]

Williams JC, Rennaker RL, Kipke DR. Long-term neural recording characteristics of wire microelectrode arrays implanted in cerebral cortex. Brain Res Protoc. 1999; 4:303–313.

Wise KD, Anderson DJ, Hetke JF, Kipke DR, Najafi K. Wireless implantable microsystems: high-density electronic interfaces to the nervous system. Proc IEEE. 2004; 92:76–97.

Xiao Y, Guo C, Li CM, Li Y, Zhang J, Xue R, et al. Highly sensitive and selective method to detect dopamine in the presence of ascorbic acid by a new polymeric composite film. Anal Biochem. 2007; 371:229–237. [PubMed: 17720131]

Yan L, Marzolin C, Terfort A, Whitesides GM. Formation and reaction of interchain carboxylic anhydride groups on self-assembled monolayers on gold. Langmuir. 1997; 13:6704–6712.

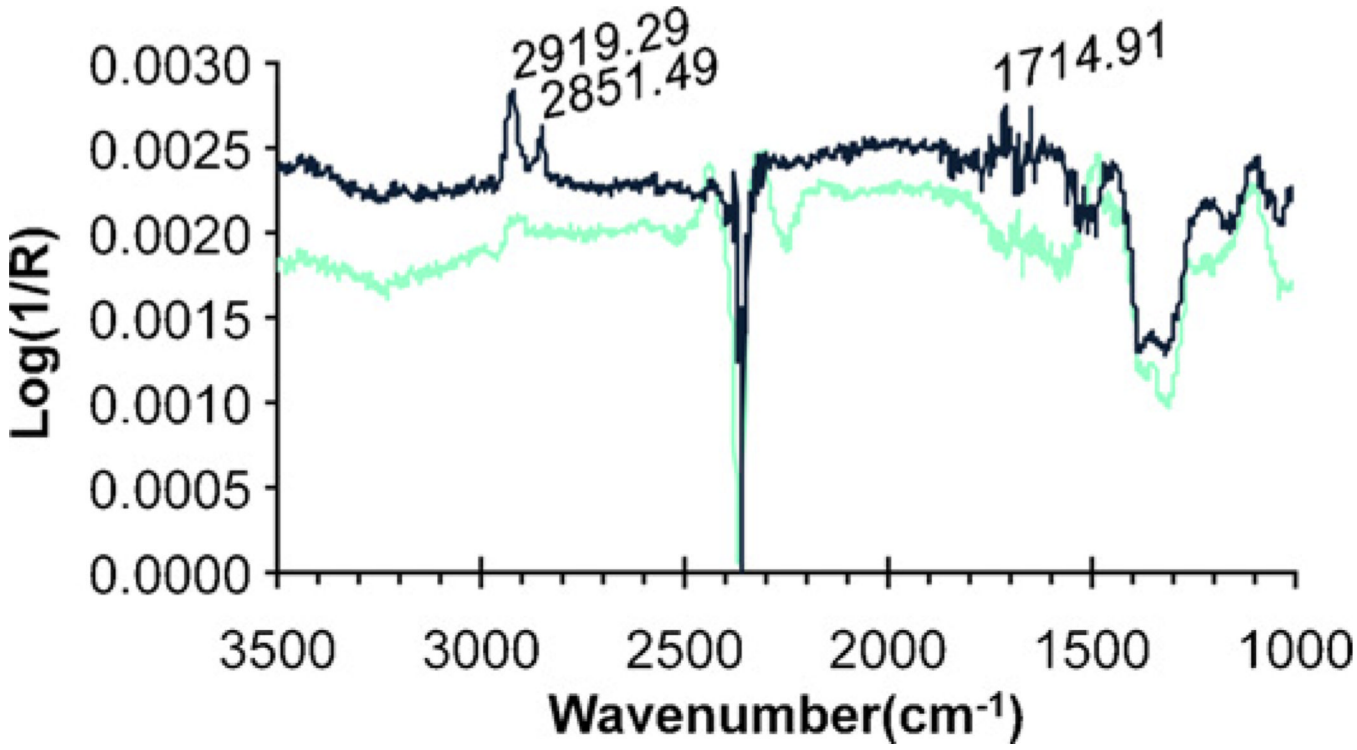

Fig. 1.
IR spectroscopy. Gray: control Si wafer coated with 100 Å Ti and 1000 Å Au. Black: Si wafer coated with 100 Å Ti, 1000 Å Au, and 11-mercaptoundecanoic acid. Three peaks are seen at wavenumbers 2919 cm^{-1}, 2851 cm^{-1}, 1714 cm^{-1}. Peaks indicate that 11-mercaptoundecanoic acid was present on the wafer and the shuttle.

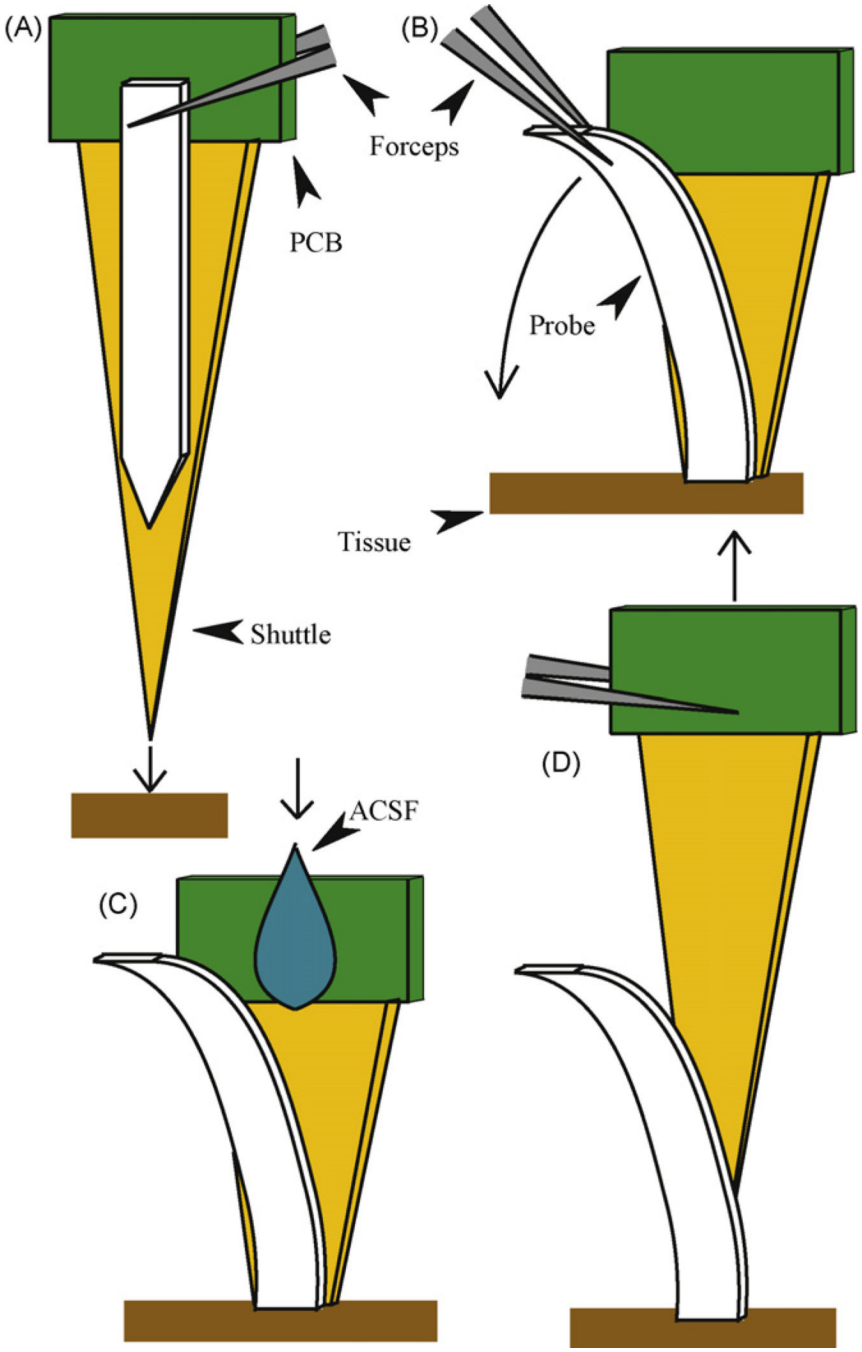

Fig. 2.

(A) The flexible probe and SAM-coated insertion shuttle were inserted together with forceps. (B) The polymer probe was then peeled from the top of the insertion shuttle to the base of the tissue surface. (C) A drop of ACSF was used to help separate the polymer from the insertion shuttle. (D) The insertion shuttle was then slowly explanted using forceps.

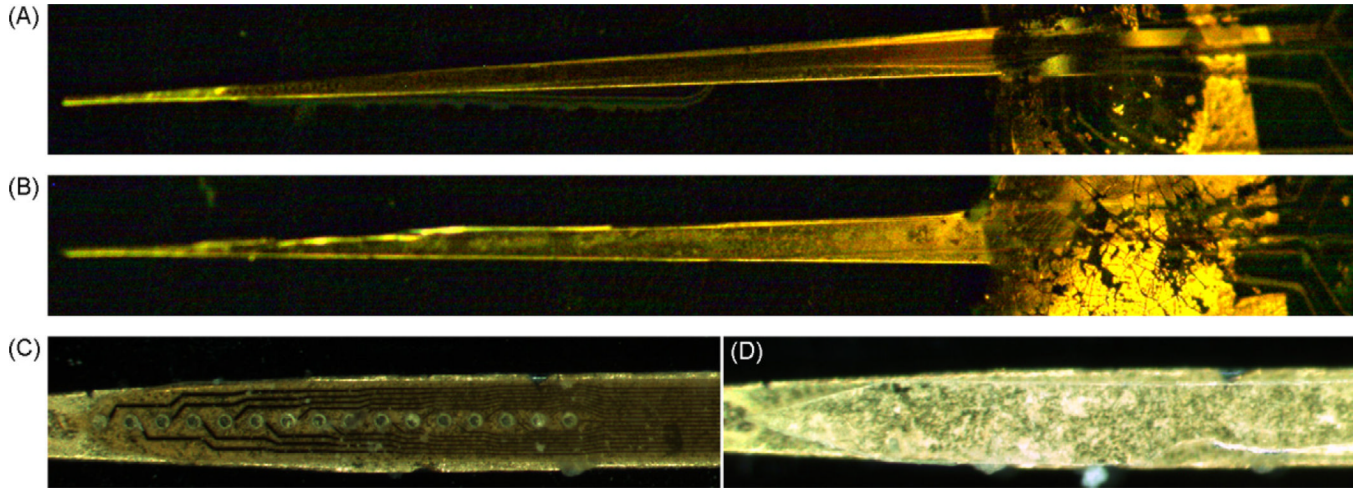

Fig. 3.
Polymer probes prepared on SAM-coated insertion shuttle. (A) 196 μm wide polyimide probe. (B) 200 μm wide PDMS probe. (C) Tip of polyimide probe on the shuttle. (D) Tip of clear PDMS probe on the shuttle, the clear PDMS probe can be identified by its white outline.

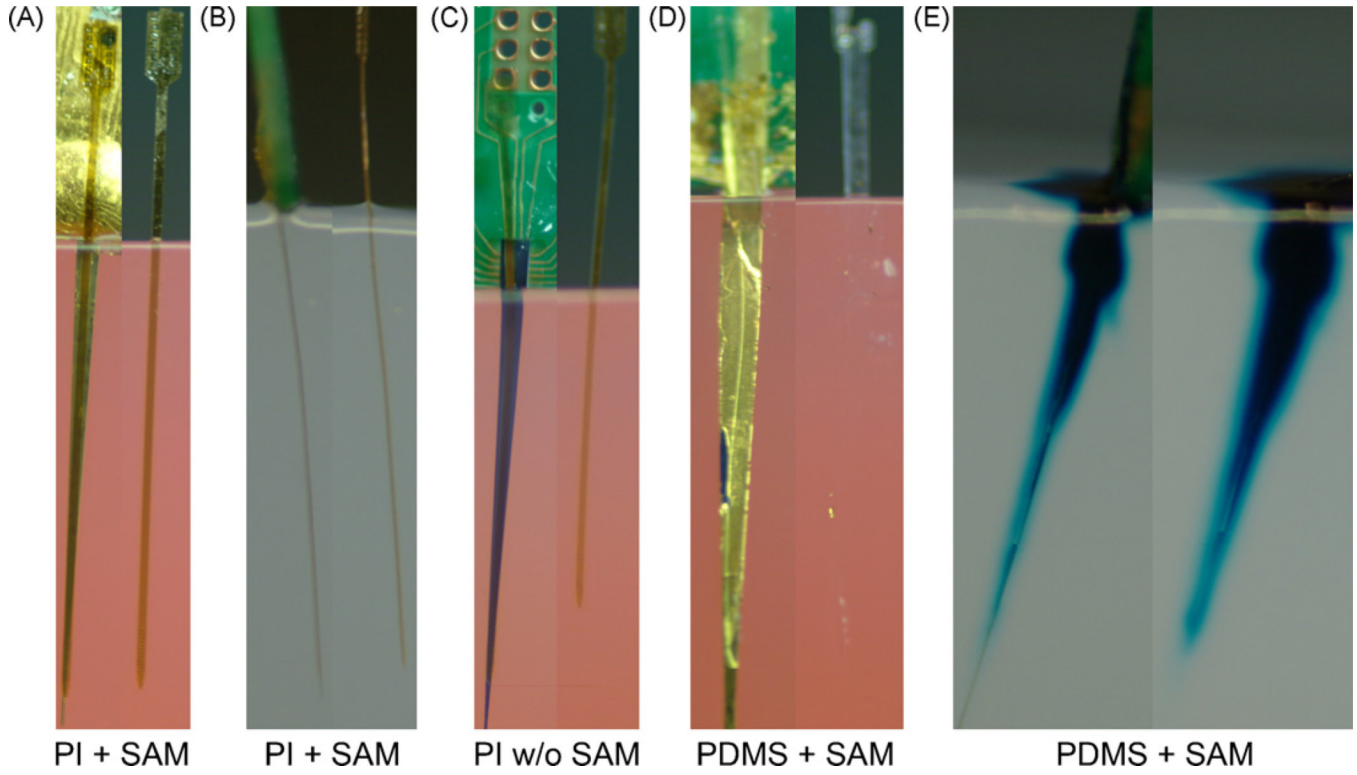

Fig. 4.

Polymer probes were inserted ~8.5 mm deep and imaged though 0.5% agarose gel. Left, after implantation, before shuttle explantation. Right, after shuttle explantation. (A–C) 196 μm wide polyimide probes. (D and E) 200 μm wide PDMS probes. (A and D) Probes implanted with the SAM-coated insertion shuttle. (B and E) Probes implanted with the SAM-coated insertion shuttle imaged from the side demonstrating no measurable deflection occurs during shuttle insertion or explantation. (C) Polyimide probe implanted with a non-coated insertion shuttle. (E) Blue dye was used to help visualize the PDMS probe. The PDMS probe can be seen as a white track in the blue dye. PDMS probes inserted with non-coated insertion shuttle resulted in explantation of the PDMS probe (not shown).

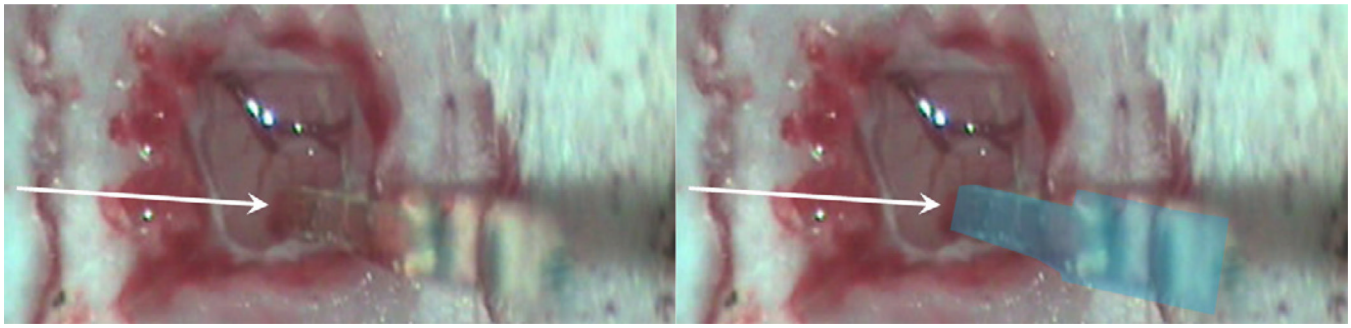

Fig. 5.

A craniotomy was made over the motor cortex. Dura was cut and folded back. A clear PDMS probe was inserted into the rat motor cortex using the insertion shuttle. Left; PDMS probe was released from the shuttle and then the shuttle was removed leaving the PDMS probe only. Arrow indicates the point of insertion. Right; shading highlights the location of the clear PDMS probe.

Table 1

Displacement of shuttle inserted polymer probes in tissue phantom during shuttle removal.

Probe	Shuttle coating	Average implant distance (μm)	Avg. % displacement ± S.E.	Avg. μm displacement ± S.E.	*N*
Polyimide	SAM	8830	1.0 ± 0.7	85 ± 55	10
Polyimide	SAM (repeat)[a]	8270	3.3 ± 1.5	299 ± 135	10
PDMS	SAM	8280	2.1 ± 1.1	167 ± 79	10
Polyimide	No coating	8830	26.5 ± 3.7	2365 ± 334	10
PDMS	No coating	8130	100.0 ± 0.0	8130 ± N/A	10

[a]Probes were implanted consecutively with a single shuttle.